Exercise 2 - Pendulum with varying length

Tom Vadot, Martin Godet
tom.vadot@epfl.ch, martin.godet@epfl.ch

March 26, 2024

Contents

1 Introduction **1**

2 Analytical results **2**
2.1 System of differential equations 2
2.2 Mechanical energy 3
2.3 Specific solution for a rod with constant length 4

3 Simulations **4**
3.1 Constant length pendulum 4
3.2 Decreasing length pendulum 5
3.3 Oscillating length pendulum 7
3.4 Poincaré map 9

4 Conclusion **10**

1 Introduction

The mass-pendulum system is a well known and often analysed system in classical mechanics. However, some assumptions are often placed on the pendulum, like a constant length or small oscillations in order to explicitly solve the equations of motion. In this report, we will approach this problem numerically, enabling us to study more complex cases. The velocity-Verlet method will be used to carry out the simulations. Along with the study of the system itself, the convergence of the algorithm under different conditions will be determined.

We will first consider the simplest system, with a constant pendulum length. Secondly, the behavior of the mass when the rod is slowly shortened will be analysed. Finally, the length of the rod will vary periodically. The first situation aims mostly at verifying that the simulation remains in line with the theory and determining the characteristics of the algorithm used. The second simulation will be analysed to verify the mechanical energy theorem: lost or gained energy is due to the power of non-conservative forces. The final setting will allow us to show the chaotic behavior of the system. The overall motion, whether periodic or chaotic, will be shown using a Poincaré map. Some analytical results will also be proven in order to verify the soundness of our simulation by comparing them to the computational results.

The velocity-Verlet method has been implemented in C++, where the simulations are then carried out. The results of the simulations were analysed using Jupyter Notebooks, which have

been included in the extra files associated with this report.

2 Analytical results

The system studied for this report is a simple pendulum of mass $m = 0.2$ kg attached to a rod of time-dependent length

$$\ell(t) = L + \alpha t + d\sin(\omega t) \tag{1}$$

where $L = 0.2$ m and the other parameters are set depending on the simulation. The mass experiences a downwards acceleration due to gravity $\vec{g} = -g\vec{e_y}$ and a tension force due to the rod $\vec{T} = T\vec{e_r}$, where $\vec{e_x}$, $\vec{e_y}$ are the basis vectors of a cartesian coordinate system centered in $\mathcal{O}$ and $\vec{e_r}$, $\vec{e_\theta}$ the basis vectors of a polar coordinate system, as shown in FIGURE 1.

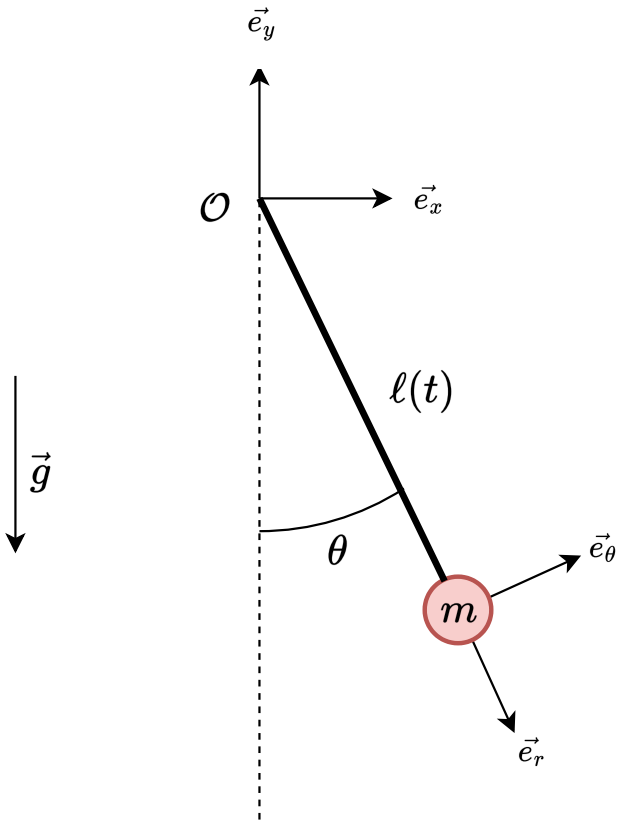

Figure 1: A simple pendulum of mass m and variable length $\ell(t)$

2.1 System of differential equations

Question (a)

Let us take the vector: $\mathbf{y} = (\theta, \dot{\theta})$

We are searching for $\mathbf{f}$ such that:

$$\frac{\mathrm{d}\mathbf{y}}{\mathrm{d}t} = \begin{pmatrix} \dot{\theta} \\ \ddot{\theta} \end{pmatrix} = \mathbf{f}(\mathbf{y}) \tag{2}$$

The forces applied on the mass expressed in the polar coordinate system $\vec{e_r}, \vec{e_\theta}$ are

$$m\vec{g} = mg\cos(\theta)\vec{e_r} - mg\sin(\theta)\vec{e_\theta} \tag{3}$$

$$\vec{T} = T\vec{e_r} \tag{4}$$

where $g = 9.81\ \mathrm{m\,s^{-1}}$ and T is the (signed) norm of the tension force. Using the formulae for acceleration in polar coordinates we obtain the following equations of motion

$$\begin{cases} m(\ddot{\ell}(t) - \ell(t)\dot{\theta}^2) = mg\cos(\theta) + T \\ m(\ell(t)\ddot{\theta} + 2\dot{\ell}(t)\dot{\theta}) = -mg\sin(\theta) \end{cases} \tag{5}$$

knowing $\dot{\ell}(t) = \alpha + d\omega\cos(\omega t)$ and $\ddot{\ell}(t) = -d\omega^2\sin(\omega t)$. By rearanging these equations, we obtain

$$\begin{cases} \dot{\theta} = \pm\sqrt{\frac{-g\cos(\theta) - \frac{T}{m} + \ddot{\ell}(t)}{\ell(t)}} \\ \ddot{\theta} = \frac{-g\sin(\theta) - 2\dot{\ell}(t)\dot{\theta}}{\ell(t)} \end{cases} \tag{6}$$

which allows us to rewrite EQUATION 2 as

$$\frac{\mathrm{d}\mathbf{y}}{\mathrm{d}t} = f(\mathbf{y}) = \begin{pmatrix} \dot{\theta} \\ \frac{-g\sin(\theta) - 2\dot{\ell}(t)\dot{\theta}}{\ell(t)} \end{pmatrix} \tag{7}$$

2.2 Mechanical energy

Question (b)

We are searching for the total mechanical energy of the system. By considering the mass as a point mass, we can write the total mechanical energy as the sum of the translational kinetic energy and the potential. The tension does not derive from any potential so it will not appear in the expression of the mechanical energy. The gravitational force is of course derived from a potential which gives:

$$\begin{aligned} \mathrm{E_{tot}} &= \frac{1}{2}mv^2 + mgy \\ &= \frac{1}{2}m(\ell(t)^2\dot{\theta}^2 + \dot{\ell}(t)^2) - mgl(t)\cos(\theta) \end{aligned} \tag{8}$$

This energy is not conserved. The energy of the gravitational potential is conserved as gravity is a central force. However, the tension does not derive from a potential and does produce work, as the mass moves along the $\vec{e_r}$ direction. This impacts the total mechanical energy that is therefore not conserved. The power of this non-conservative force is given by:

$$\begin{aligned} P &= \vec{T}\cdot\vec{v} \\ &= T\dot{\ell}(t) \end{aligned} \tag{9}$$

Using the first equation from EQUATION 5, we can express T as

$$T = m(\ddot{\ell}(t) - g\cos(\theta) - \dot{\theta}^2\ell(t)) \tag{10}$$

which gives us the final expression for the power

$$P = m(\ddot{\ell}(t) - g\cos(\theta) - \dot{\theta}^2\ell(t))\dot{\ell}(t) \tag{11}$$

2.3 Specific solution for a rod with constant length

Question (c)

For this part we will set $\alpha = 0$ and $d = 0$, meaning the length of the pendulum remains constant ($\ell(t) = L$). We assume small movements around the stable equilibrium position, i.e. $\theta \ll 1$. Under this assumption, we can write $\sin(\theta) \approx \theta$ and $\cos(\theta) \approx 1$. The equations of motion from EQUATION 5 then become:

$$\begin{cases} -mL\dot{\theta}^2 = mg\cos(\theta) + T = mg + T \\ mL\ddot{\theta} = -mg\sin(\theta) = -mg\theta \end{cases} \tag{12}$$

from which we get

$$\ddot{\theta} = -\underbrace{\frac{g}{L}}_{\omega_0^2}\theta \tag{13}$$

which is the equation for a harmonic oscillator with pulsation $\omega_0 = \sqrt{g/L}$. The general solution is given by

$$\theta(t) = A\cos(\omega_0 t) + B\sin(\omega_0 t) \tag{14}$$

Imposing the intial conditions $\theta(0) = \theta_0$ and $\dot{\theta}(0) = 0$, we find $A = \theta_0$ and $B = 0$. The solution for this case is thus given by:

$$\theta(t) = \theta_0\cos(\omega_0 t) \tag{15}$$

which gives:

$$\dot{\theta}(t) = -\theta_0\omega_0\sin(\omega_0 t) \tag{16}$$

3 Simulations

3.1 Constant length pendulum

In this first part, we will consider the case where $\alpha = 0$ and $d = 0$, that is the length of the pendulum remains constant $\ell(t) = L$. This corresponds to the situation analysed in SUBSECTION 2.3. Using a small initial angle of $\theta_0 = 10^{-10}$ and no initial speed, a convergence study of the final angle and angular speed of the velocity-Verlet method was done. Comparing the final position and angular speed obtained numerically with the analytical results in EQUATION 15 and EQUATION 16, we obtain an error on the final position and angular velocity. The results in FIGURE 2 show that the orders of convergence of this method, for these initial conditions, are 4 and 2 for the position and velocity respectively.

Varying the initial angle θ_0 between 0 and π allows us to get larger movements from the pendulum, as shown in FIGURE 3A. The angular frequency was extracted by looking at the time elapsed between the starting condition and the time it takes for two sign changes in angular speed (otherwise we would be measuring a half-period). Writing that time as T, the period of oscillation, we get the angular frequency $\Omega = \frac{2\pi}{T}$. The results are shown in FIGURE 3B. These results are coherent with the physical reality, as a larger angle should correspond to a longer oscillation period than a smaller angle. It is interesting to note that the angular frequency does not change linearly, which is consistent with the results measured in the lab: small angles have less effect than large angles.

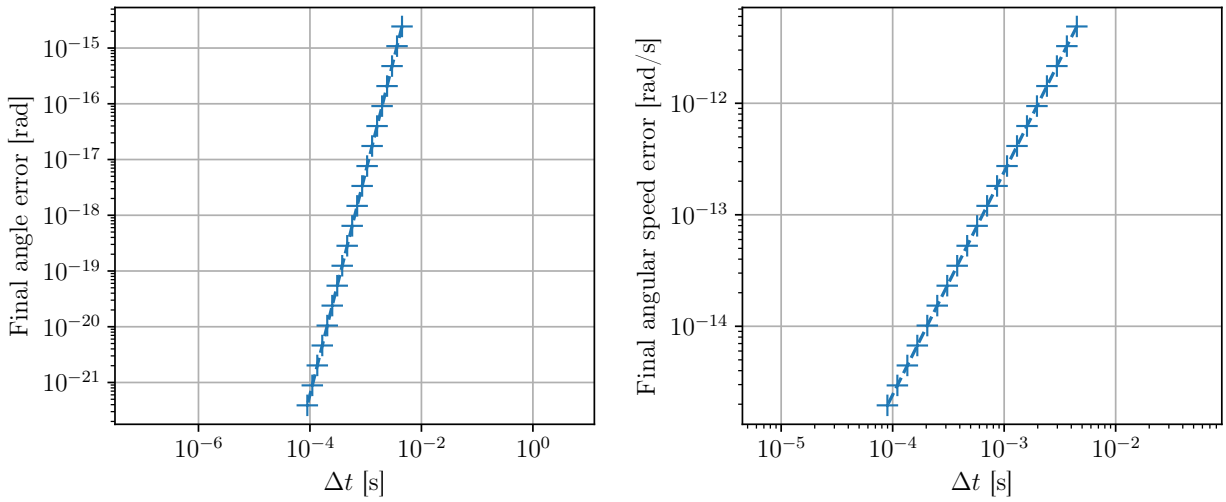

(a) Position (angle of pendulum)

(b) Angular velocity

Figure 2: Numeric convergence of different variables for initial conditions $\theta_0 = 10^{-10}$, $\dot{\theta}_0 = 0$ s^{-1} and simulated until $t_{\text{fin}} \approx 2.69$ s, corresponding to 3 periods of oscillation

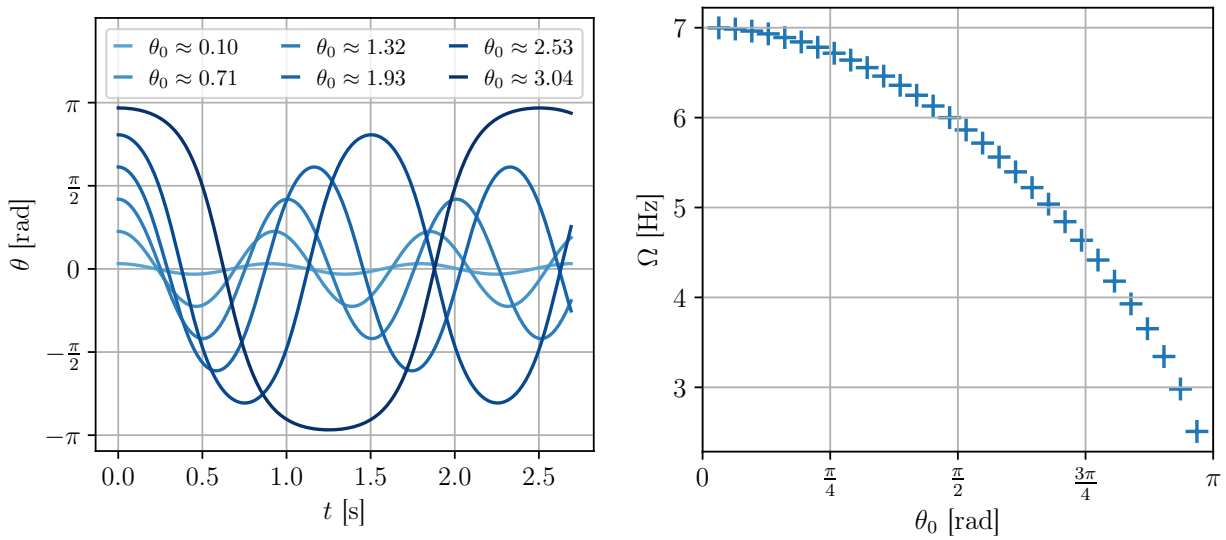

(a) Time evolution

(b) Angular frequency

Figure 3: Time evolution and angular frequency for multiple starting angles ($n_{\text{steps}} = 10000$)

3.2 Decreasing length pendulum

The next simulations were run with conditions $\alpha = -0.02$ m s^{-1} and $d = 0$ m and up to $t_{\text{fin}} = 0.96L/|\alpha|$ in order to show the behavior of the mass when its rod has a length decreasing almost to 0. First a convergence analysis was done to determine the characteristics of the algorithm when used under these conditions. The various final positions for a given time step Δt are shown in FIGURE 4. Taking the time step squared show the points aligning which indicates that the velocity-Verlet algorithm converged in order 2 for this simulation. Extrapolating from this line, we get that the algorithm converges in order 2 towards $\theta \approx 78.381$ This already indicates a greater instability of the system compared to the classical harmonic oscillator.

The first step in studying this system is understanding conceptually how it behaves. As shown

in FIGURE 5A the oscillations remain low until close to the end of the simulation, corresponding to a very short rod for the pendulum, where they explode.

The values in radians going up to 80 show that in the simulation the pendulum stops oscillating aroung its stable equilibrium and rather does complete rotations around the center $\mathcal{O}$. This is coherent with the fact that it will have not only gained mechanical energy with the work from the tension T but as the rod gets shorter less energy is required to do a complete rotation. The phase space in FIGURE 5B also shows the small oscillations followed by an explosion towards higher values of θ and $\dot{\theta}$.

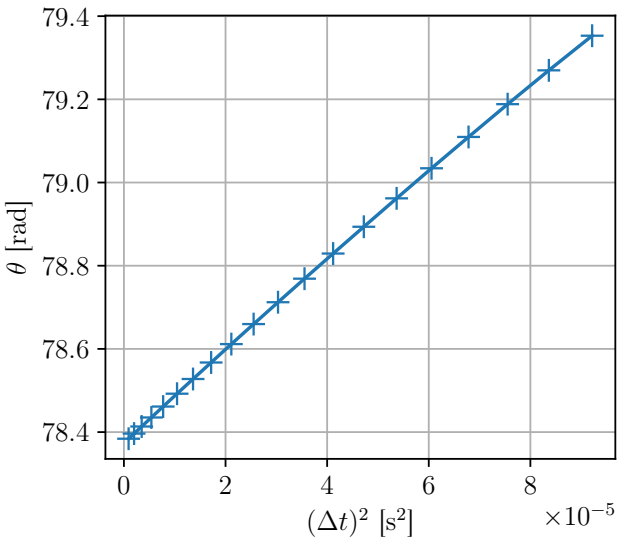

Figure 4: Convergence of the velocity-Verlet algorithm for a pendulum with decreasing length, initial conditions: $\theta_0 = 0.5$, $\dot{\theta}_0 = 0$ s^{-1}

A final physical point of interest is the energy of the system. We want to verify if the algorithm respects the theorem of mechanical energy $\mathrm{d}E_{mec}/\mathrm{d}t = P_{\text{nonc}}$ with P_{nonc} the power from non-conservative forces. The FIGURE 6A and FIGURE 6B show that this theorem is perfectly verified in this simulation. The FIGURE 6A in particular illustrates that the variation of the energy in time, calculated through centered differences, is exactly the power without any visible differences. This can also be illustrated by integrating the power, this is done by summing the small $\mathrm{d}P = P_{\text{nonc}}\mathrm{d}t$, and showing as in FIGURE 6B that substracting it to the energy gives a constant.

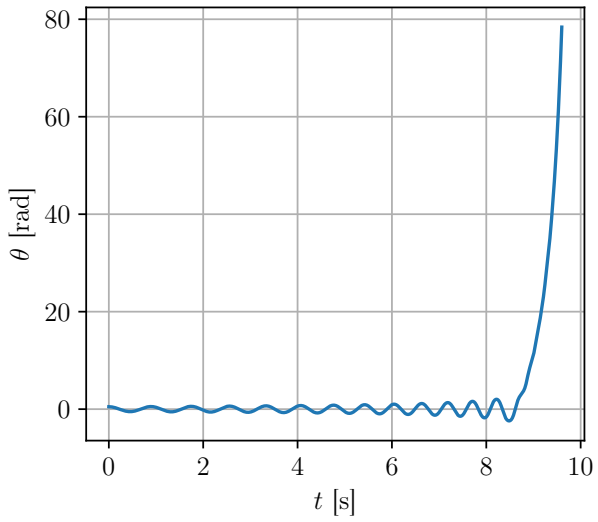

(a) Time evolution

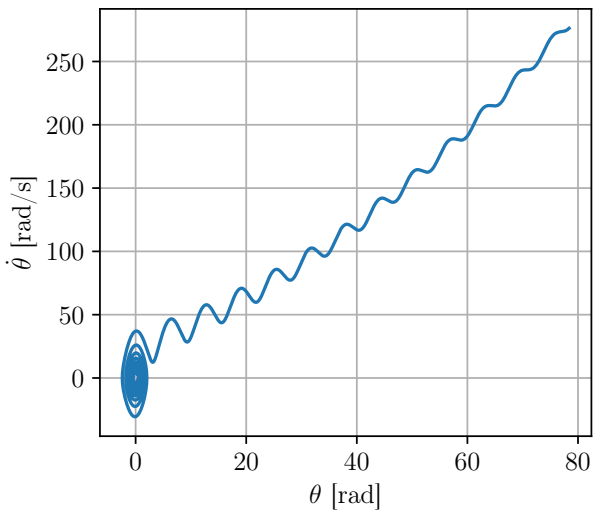

(b) Phase space

Figure 5: Time evolution and phase space of a pendulum with decreasing length during $n_{\text{steps}} = 10000$; initial conditions: $\theta_0 = 0.5$, $\dot{\theta}_0 = 0$ s^{-1}

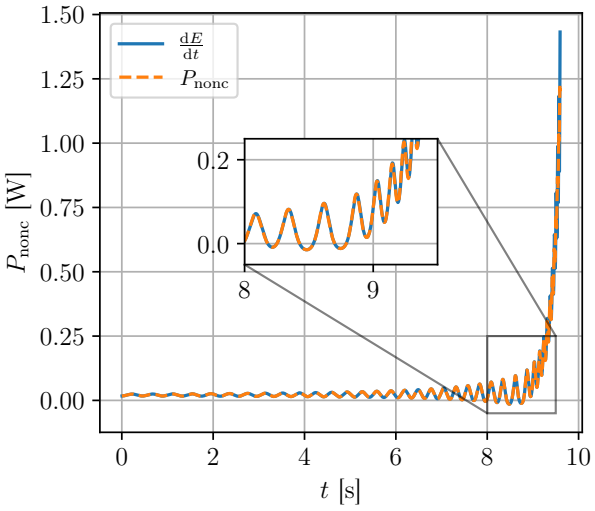

(a) Power

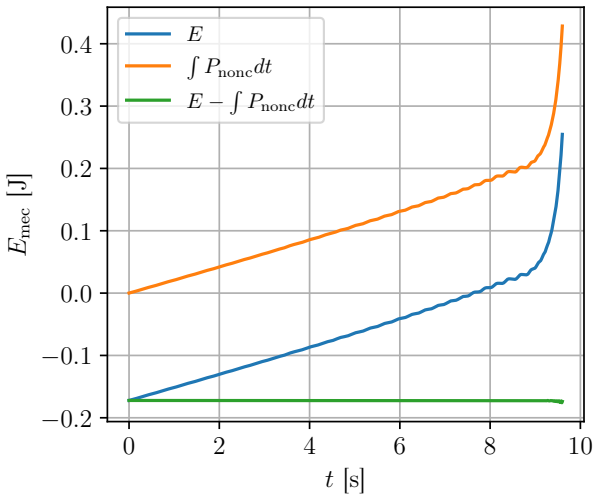

(b) Energy

Figure 6: Theorem of mechanical energy for a pendulum with decreasing length; initial conditions: $\theta_0 = 0.5$, $\dot{\theta}_0 = 0$ s^{-1}; $n_{\text{steps}} = 2000$

3.3 Oscillating length pendulum

The final case study concerns the conditions $\alpha = 0$ m s^{-1}, $d = 0.01$ m and $\omega = 2\omega_0 = 2\sqrt{g/L}$ as calculated in SUBSECTION 2.3.

Taking small oscillations, $\theta_0 = 0.01$, we can illustrate the behavior of an excited oscillator as shown in FIGURE 7. This simulation was run for 200 periods of the oscillation of the length $T_{\text{excit}} = 2\pi/\omega$. This corresponds numerically to two large oscillations of the amplitude of the smaller oscillations. This behavior indicates that the excitations increase the energy to a maximum, giving larger oscillations, and then start working against it to bring it back to a minimum.

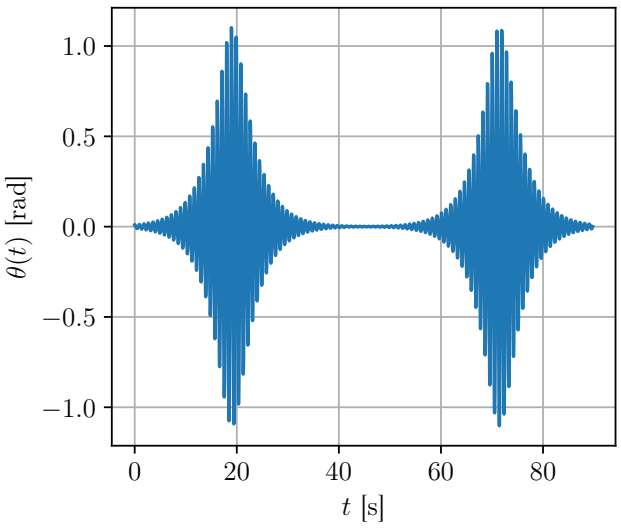

Figure 7: Time evolution of an oscillator excited through varying the length of its rod; initial conditions: $\theta_0 = 0.01$, $\dot{\theta}_0 = 0$ s^{-1}; $n_{\text{steps}} = 1000$ per period of excitation

An interesting feature of this new system is the chaotic behavior it can present by taking larger oscillations. We first need to analyse the convergence of our algorithm in this new chaotic system. As can be seen in FIGURE 8A the velocity-Verlet algorithm still converges correctly in order 2 for 10 periods of excitation. In this given simulation the final value towards which the algorithm converges in order 2 is $\theta(10T_{\text{excit}}) = 39.071175$ obtained through a linear fit on the aligned points and evaluated at $\Delta t = 0$. However after too many excitations as shown in FIGURE 8B, here 20 periods, with a decreasing Δt the final position does not converge to a single value in any polynomial order. It oscillates slightly due to the chaotic nature of the system.

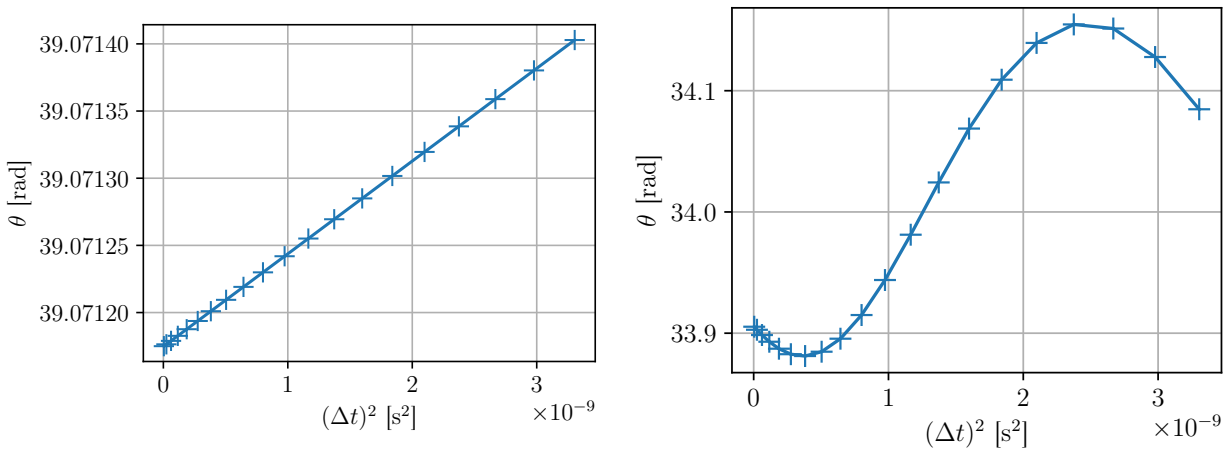

(a) 10 periods

(b) 20 periods

Figure 8: Convergence of the velocity-Verlet algorithm for a chaotic system and different numbers of periods of excitation; initial conditions: $\theta_0 = 0$, $\dot{\theta}_0 = 15$ s^{-1}

To further illustrate the chaos in this system we can show the strong dependence on initial conditions. The distance δ represented in FIGURE 9 was calculated with the formula:

$$\delta(t) = \sqrt{\omega_0^2(\theta_1(t) - \theta_2(t))^2 + (\dot{\theta}_1(t) - \dot{\theta}_2(t))^2} \tag{17}$$

It represents a type of distance between two trajectories during 40 periods of excitation, θ_1 and θ_2, corresponding respectively to the initial conditions $\theta_{0,1} = 0$, $\dot{\theta}_{0,1} = 15$ s^{-1} and $\theta_{0,2} = 10^{-6}$, $\dot{\theta}_{0,2} = 15$ s^{-1}. These two very close initial conditions give diverging trajectories as illustrated by the growth of the distance δ. This represents an exponential growth of the divergence of the trajectories. This exponential has the exponent of Lyapounov: $\lambda \approx 0.76$. This allows to characterise the chaos of this system by knowing the rate of growth of the divergence of trajectories with similar starting conditions.

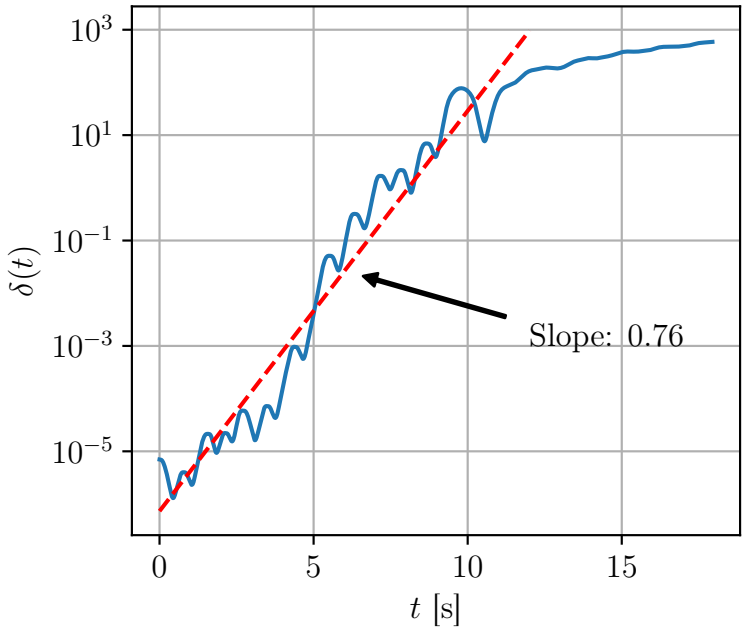

Figure 9: Distance in the phase space between two chaotic trajectories for an oscillator with varying length, indication of the Lyapounov exponent, $n_{\text{steps}} = 10000$ per period of excitation

3.4 Poincaré map

The same chaotic system can be sampled more clearly through a Poincaré map. To achieve this we run the simulation with a number of steps $n_{\text{steps}} = 1000$ per period of excitation and we sample the phase space at every period. The FIGURE 10 shows the results for 11 initial conditions and 30 000 periods. We see that for certain small enough values of the initial energy we have a simple Poincaré map representing a non-chaotic system. This is illustrated with the conditions going up to $\theta_0 = 0$, $\dot{\theta}_0 = 12.13\ \text{s}^{-1}$. For these conditions the system will show a behavior similar to the one obtained in FIGURE 7. A difference that can be noted between these non-chaotic systems is that the one with $\theta_0 > 0$, $\dot{\theta}_0 > 0$ has a jump between two symetrical parts of the system close to the origin. This represents a phase with the excitations such that it never reaches small values of θ or $\dot{\theta}$ at the end of an excitation period. Some other non-chaotic conditions do not approach the origin of the phase space ($\theta = 0, \dot{\theta} = 0$) representing oscillations for which the tension does not produce enough work against to bring them to small energies.

We can observe two boundary conditions, still on FIGURE 10, at $\dot{\theta}_0 = 11.88\ \text{s}^{-1}$ and $\dot{\theta}_0 = 12.13\ \text{s}^{-1}$. These boundary conditions are non-chaotic. The first one gives small "islands" representing a certain phase with the excitations. The second one is the closest value found to the limit before reaching chaotic systems. Any test simulation run with greater initial energies than for this one led to chaotic systems.

Above this treshold of initial energy the system becomes chaotic and samples the same shape shown by the two different chaotic systems in the FIGURE 10. This shows that the chaos is not pure randomness but instead it samples a certain precise part of the phase space in a seemingly random way, that is underneath deterministic according to classical mechanics. A final simulation with a very large $\dot{\theta}_0$, here $20\ \text{s}^{-1}$, was run and it shows that at some point very fast rotations do not leave enough freedom for the oscillations of the length to play a big part in the system. The system simply rotates very fast around $\mathcal{O}$ and is not chaotic anymore.

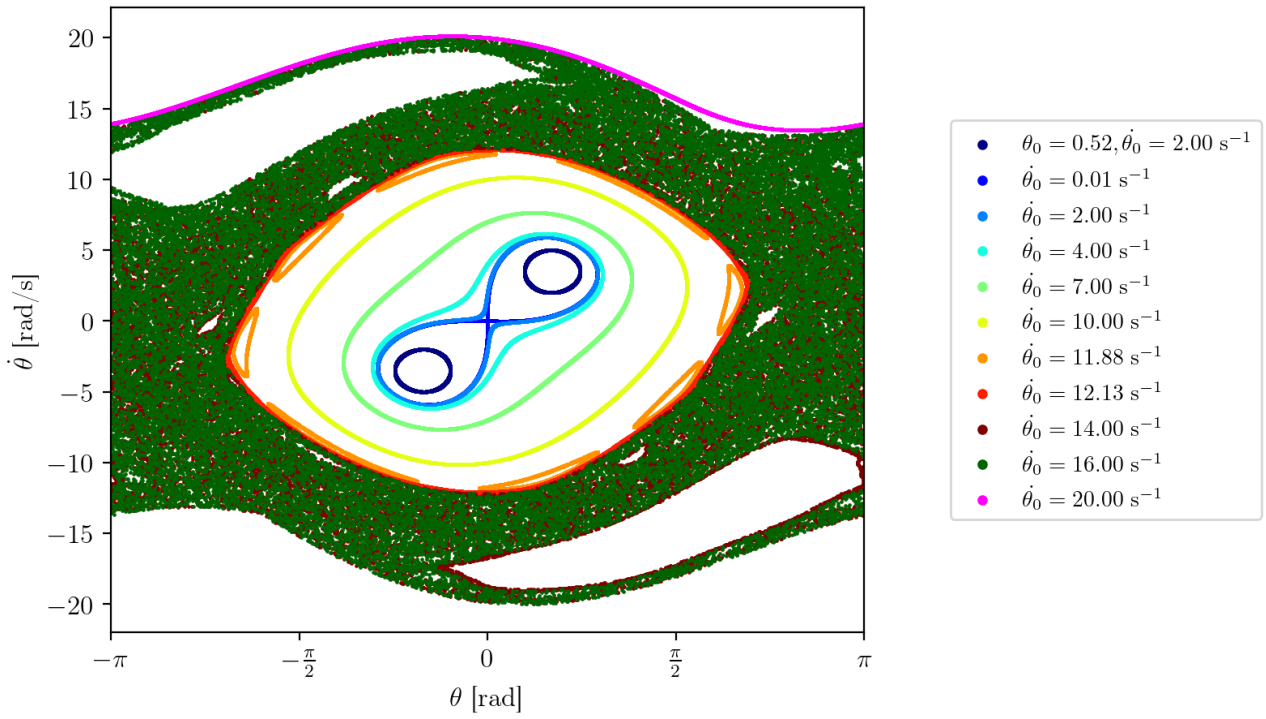

Figure 10: Poincaré map of a chaotic system, a pendulum with varying length, for various initial conditions, $\theta_0 = 0$ unless said otherwise ($n_{\text{steps}} = 1000$, $N = 30000$ periods of excitation)

4 Conclusion

In this report the pendulum with constant and varying length was analysed numerically in great detail. The first results for constant length showed the great precision of the velocity-Verlet method and its good convergence, of order 4 for the position. The obtained results were very coherent with the analytical ones with errors as small as 10^{-18}. Knowing that this algorithm gives good results it was possible to simulate more complex cases starting with a decreasing length for the pendulum. The order of convergence was affected negatively but this still allowed to see a behaviour coherent with our physical intuition. Despite even the explosion in the angular values the theorem of mechanical energy was verified which gives another indication of the great precision of this numerical method. The last conditions that were analysed were for an oscillating length of the rod. This gave forced oscillators for small oscillations but a chaotic system above a certain treshold of energy. In this chaotic case the linear convergence was not verified anymore and the trajectories became very dependent on the initial conditions. Poincaré maps were used to illustrate the phase space of chaotic and non-chaotic cases which gave a few final informations about the physical behavior of the system.

This study thus allows to confidently use the velocity-Verlet method to simulate oscillators even in non-conventional and chaotic cases. It is also a great tool to determine the characteristics of the oscillations in these cases.